

## SYNTHESIS AND CHARACTERIZATION OF CdS IN DIOL VANILIN LIQUID CRYSTAL MONOMER

H.L. Lee<sup>1</sup>, M. Abu Bakar<sup>1,\*</sup>, J. Ismail<sup>1</sup> and A.M. Issam<sup>2</sup>

<sup>1</sup> Nanoscience Research Laboratory, School of Chemical Sciences, University Sains Malaysia, 11800 Penang, Malaysia

<sup>2</sup> School of Industrial Technology, University Sains Malaysia, 11800 Penang, Malaysia

Received 30 March 2007; Accepted 20 June 2007

### ABSTRACT

Nanocomposites comprising diol-vanilin and cadmium sulfide (CdS) has been synthesized via chemical precipitation method in ethanol at refluxed temperature (160 °C) for 12 hours. CdCl<sub>2</sub>. 2.5H<sub>2</sub>O and thiourea as cadmium and sulfide precursors respectively were employed. Diol vanilin is a thermotropic liquid crystal monomer which exhibits enantiotropic nematic metaphase texture when observed under polarizing microscope and confirmed by DSC thermal stability study. A series of different mass composition of diol vanilin and CdS nanocomposites ranging from 0.1:1.0 till 1.0:1.0(w/w) were prepared and characterized using XRD, TEM, SEM-EDX, POM and DSC. The X-ray diffraction pattern (XRD) showed broad peaks due to the formation of cubic CdS nanoparticles in diol vanilin matrix. The nanocomposites at low mass composition of CdS still maintained their nematic phase. However, the liquid crystal property was affected when the mass composition of CdS in nanocomposite was increased and the liquid crystal characteristic vanished when the mass composition was at 0.6:1.0.

**Keywords:** CdS, diol vanilin, thermotropic liquid crystal, nanocomposite.

### INTRODUCTION

The inorganic/organic nanocomposites have attracted great interest from the researchers due to their novel optical and electronic properties [1]. This could be attributed to the quantum confinement effect, nonlinear optical behaviors and the large ratio of surface to volume of these nanocrystals [2]. The nanocomposites exhibit controlled inorganic crystallite size [3] as well as the morphology. Most studied of inorganic/organic nanocomposites belong to the II-VI group and metal chalcogenides such as CdS. CdS has a wide spread applications in the field of electronics ranging from phosphors to photovoltaic cells. Two steps were generally required to synthesize metal sulfide in organic nanocomposites. Metal ions were initially introduced into an organic monomer and then a sulfur source was added for the preparation of nanocrystalline sulfide. Various preparation methods have been developed; (a) a control of particle growth using stabilizers or matrices like surfactant [4], phosphine oxides, polymers, reverse micelles, vesicles, LB films, multilayer film, xerogels and silica, (b) size fractionation by exclusion chromatography or gel electrophoresis, (c) size selective chromatography [5].

In the past decades, many semiconductor/organic nanocomposites, such as CdS/poly vinyl alcohol [6], CdS/*N*-polyvinylcarbazole [7] and CdS/polystyrene [8], had been synthesized via a variety of methods. Nevertheless, there were a few reports on the incorporation of nanoparticles in liquid-crystalline polymer.

Several researchers [9, 10] have studied organoclay nanocomposites based on thermotropic liquid-crystalline polymer. In the most of the reported work, common polymers such as epoxy resin, polystyrene and polyvinyl alcohol (PVA) are often used as the matrix in the nanocomposites with CdS nanoparticles. However, to our best knowledge, no other researcher has reported on incorporation of CdS nanoparticle in thermotropic liquid crystal monomer even though Khiew and co-researchers [11, 12] have studied on synthesizing PbS and CdS nanoparticles in lyotropic liquid crystal using reverse microemulsion technique. In this paper, we report a simple chemical precipitation method to synthesize CdS in a nematic enantiotropic liquid crystal diol vanillin. Diol vanilin was synthesized from bisphenol N,N'-bis(4-hydroxy-3-methoxy)-benzylidene-*o*-tolidine with 1-chloro-6-hexanol.

### EXPERIMENTAL SECTION

#### Materials

Unless otherwise stated, all chemicals were commercially obtained and were used without further purification or distillation. The starting materials for the synthesis of CdS were CdCl<sub>2</sub>.2.5H<sub>2</sub>O (Sigma-Aldrich, USA) and thiourea (Laboratory Chemical Co.). Absolute ethanol and sodium hydroxide were obtained from System, Malaysia and Mallinckrodt Baker Inc., USA respectively. *p*-hydroxybenzaldehyde (Sigma-Aldrich, Germany), vanilin, *o*-tolidine (Fluka,

\* Corresponding author. Tel/Fax : 604-657 4854  
Email address : bmohamad@usm.my

Germany), 1-chloro-6-hexanol, sodium carbonate Fluka (Germany), absolute ethanol (System®, Malaysia) dimethylformamide (Fisher Scientific, UK), 1-butanol (Merck, Germany) and diethyl ether (Lab Scan, Thailand) were purchased. Doubly distilled water was used throughout the experiment.

### Characterization

All samples were characterized by powder X-ray Diffraction (XRD). Data were collected on a SIEMENS D5000 X-ray diffractometer with monochromatic Cu-K $\alpha$  ( $\lambda = 1.5405 \text{ \AA}$ ) radiation filter in the  $2\theta$  range of  $0-100^\circ$ . Micrographs were obtained using a Philips CM12 using transmission electron microscope operating at 80 kV. 1 mg of the sample was dispersed in 3 mL of doubly distilled water and sonicated for 5 min. A few drops of dispersion were placed on a carbon coated copper grid and the solvent was evaporated off. A scanning electron microscope-energy dispersive X-ray (SEM-EDX) model Leica Cambridge S360 was used to observe the morphology and elemental composition of the product. The powders were mounted onto the metal holder through a double-sided tape and then coated with gold. The particle size of the sample was analysed using AnalySIS Docu Image Analyzer Ver. 3.1, GmbH, Germany. FT-IR spectra were measured on a Perkin-Elmer 2000 FTIR with a potassium bromide (KBr) beam splitter. Differential scanning calorimetry (DSC) measurements were carried out with a Perkin-Elmer DSC7 series at heating rate at  $5^\circ \text{C min}^{-1}$  in nitrogen starting from  $50 - 200^\circ \text{C}$  for diol vanillin. Melting point was obtained based on the peak of the melting temperatures from DSC analysis. The liquid crystalline mesophase was determined using a polarizing optical microscope (POM) Nikon Elipse E600 equipped with Linkam THMS 600 hot stage, Linkam TP93 temperature controller and Linkam LNP cooling system (pump).

### Methods

#### Preparation of CdS

Solution A was prepared by dissolving 24 mg of cadmium chloride ( $\text{CdCl}_2 \cdot 2.5\text{H}_2\text{O}$ ) and 48 mg of thiourea ( $(\text{NH}_2)_2\text{CS}$ ) into 30 mL of ethanol in a flask under

magnetic stirring at  $160^\circ \text{C}$  in the oil bath. Solution B was prepared by dissolving 10 mg of sodium hydroxide (NaOH) in 10 mL ethanol. Then, 10 mL of solution B was rapidly pipetted into the solution. The mixed solution was held under reflux at  $160^\circ \text{C}$  for 10 h. A white precursor was formed upon mixing of solution B into solution A. The precipitates was collected by centrifugation and washed repeatedly with doubly distilled water before being dried in the vacuum oven at  $50^\circ \text{C}$  for 24 hours. The product was then used for characterization work.

#### Preparation of bisphenol *N,N'*-bis(4-hydroxy-3methoxy)-benzylidene-*o*-tolidine (I)

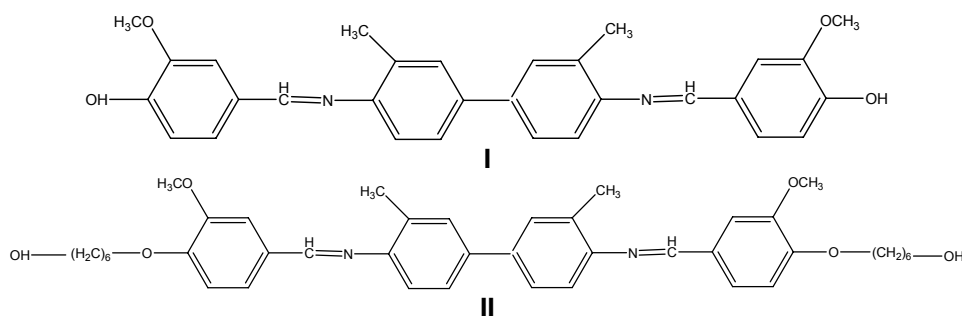
Bisphenol *N,N'*-bis(4-hydroxy-3methoxy)-benzylidene-*o*-tolidine was prepared with 0.1 mol of vanillin added drop wisely into solution of 0.05 mol *o*-tolidine in absolute ethanol. The mixture was refluxed for 6 hours with stirring. The product was then filtered, washed several times with diethyl ether and dried in the vacuum oven at  $70^\circ \text{C}$ . Final purification was carried out by re-crystallization using 1-butanol.

#### Synthesis of diol vanillin (II)

A 0.4-mol of 1-chloro-6-hexanol and 0.45 mol of sodium carbonate were mixed in 400 ml of DMF. Then, 0.2 mol of the bisphenol *N,N'*-bis(4-hydroxy-3methoxy)-benzylidene-*o*-tolidine (I) in 60 mL DMF was added together with the above mixture in the 500 ml reaction flask. The mixture was then stirred and refluxed at  $130^\circ \text{C}$  for 12 hours. The product was precipitated by pouring the obtained solution into 2 liter cold distilled water. The precipitation was then filtered, washed several times with diethyl ether and dried in the vacuum oven at  $90^\circ \text{C}$ . Final purification was carried out by re-crystallization using the mixture solvent of DMF: 1-butanol (1:1) to give light green crystals.

#### Preparation of (1.0:1.0 w/w) CdS/diol vanillin composite

A 24-mg of cadmium chloride ( $\text{CdCl}_2 \cdot 2.5\text{H}_2\text{O}$ ) and 24-mg of diol vanillin were dissolved in 15 ml of ethanol. Solution A was prepared by dissolving 12 mg of sodium hydroxide (NaOH) in 12 mL ethanol.



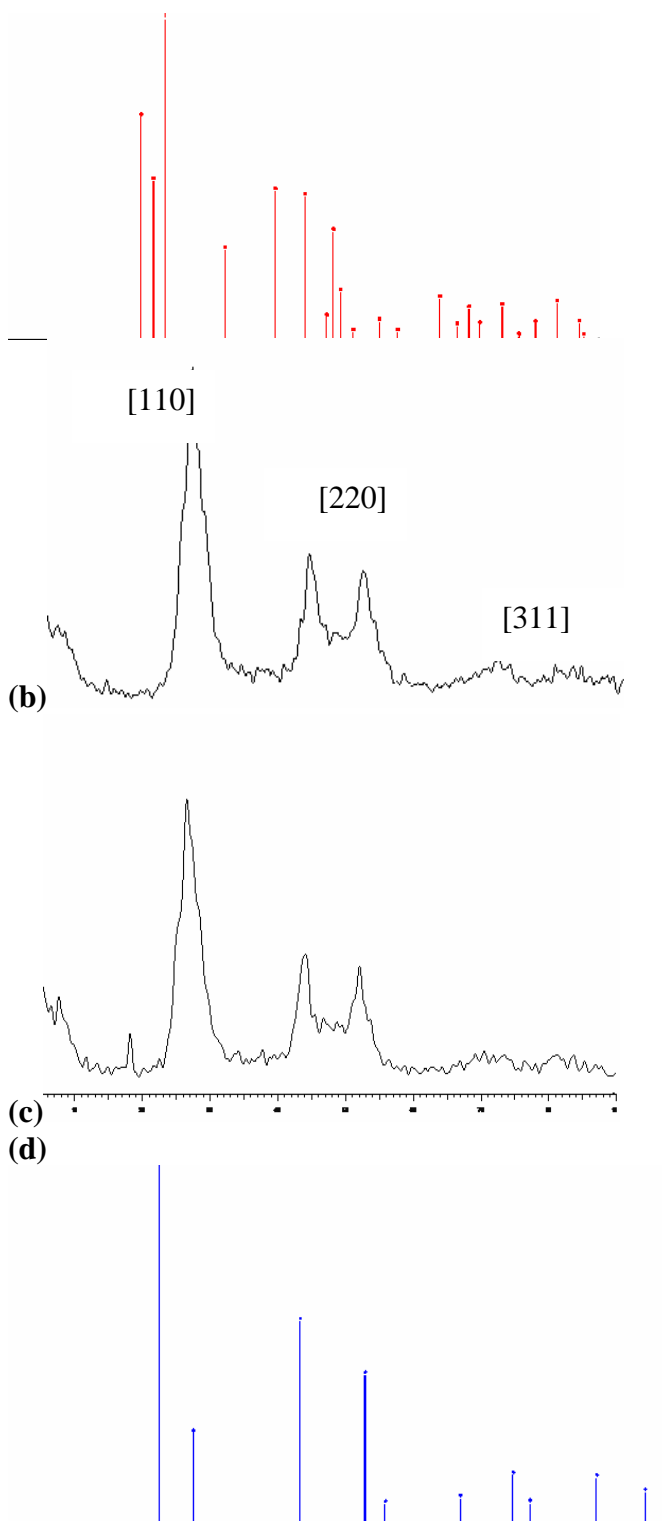


**Fig 1.** X-ray diffraction pattern of (a) hexagonal CdS (JCPDS 01-080-0006) (b) as-prepared CdS nanoparticles (c) as-prepared CdS in nanocomposites (1.0:1.0 w/w) (d) cubic CdS (JCPDS 03-065-2887)

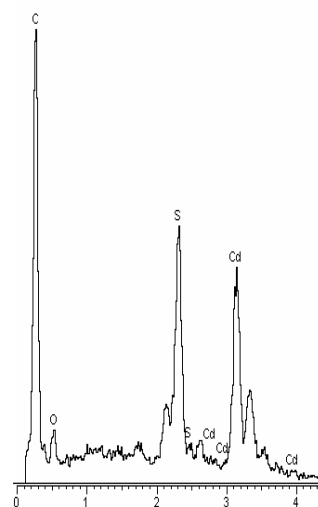


**Fig 2.** The EDX pattern of nanocomposite (1.0:1.0 w/w)

Ten milliliters of solution A was added in the mixture and stirred refluxed at 160 °C in the oil bath for 12 h. A 48 mg of thiourea ( $(\text{NH}_2)_2\text{CS}$ ) in 15 mL of ethanol and was added drop wise during the reaction. The obtained nanocomposite was collected by centrifugation and washed repeatedly with ethanol before drying in the vacuum oven at 50 °C for 24 hours. The products were then used for characterization work. A series of different mass composition of CdS to diol vanillin, were also prepared and characterized accordingly.

Fig 1 shows the XRD pattern of the as-synthesized CdS nanoparticles and nanocomposites at the mass composition of 1.0:1.0. The pattern obtained for the as-prepared CdS and the nanocomposites correspond to pure cubic CdS when compare with the standard reference (JCPDS 03-065-2887). The three peaks with  $2\theta$  values of 26.6, 44.0 and 52.0 for both samples are assignable to the three Miller indices of (111), (220) and (311). The broad peaks in the diffractogram indicate that the dimension of CdS nanoparticles are small.

The product composition was characterized by SEM-EDX analysis. The EDX pattern for CdS powder obtained is shown in Fig 2 suggest the presence of elemental Cd, S, C and O. The atomic ratio of Cd:S is 11.05:10.75 which can be translated into stoichiometric ratio of approximately 1:1. The result obtained agrees with the formulation and formation of CdS. The presence of C and O are attributed to diol-vanillin matrix in this nanocomposite. The sample is observed to have near spherical particles and the overall morphology of the particles is almost homogenous as shown in Fig 3.

Fig 4 shows the FT-IR spectra of the nanocomposites synthesized with different mass compositions. FT-IR spectrum of pure diol vanillin (Figure 4(i)) shows the absorption band at  $1618\text{cm}^{-1}$ ,

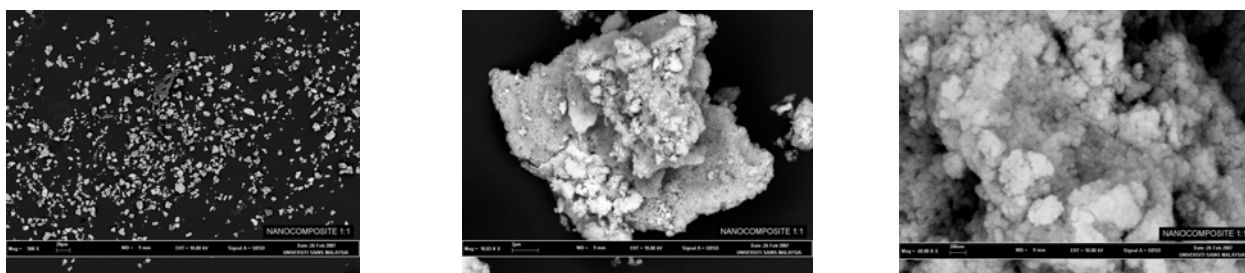


Fig 3. SEM images of as-prepared nanocomposites (1.0:1.0 w/w)

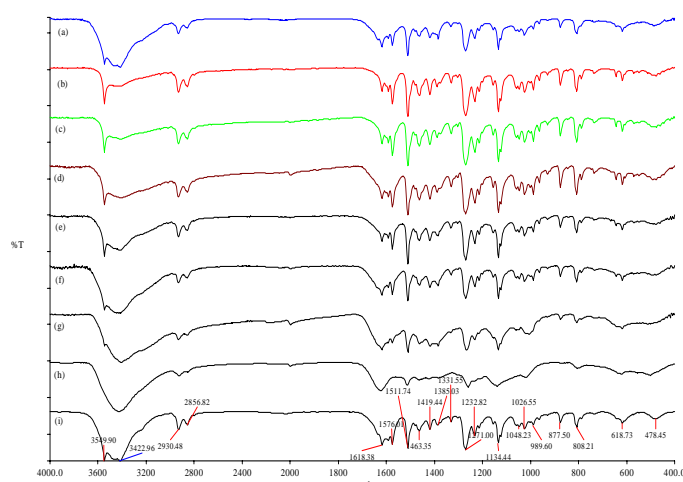


Fig 4. FT-IR spectra for nanocomposite of (a-h) mass composition of 0.1:1.0 till 1.0:1.0 w/w (CdS: diol vanillin) and (i) pure diol vanillin

indicating the presence of azomethine,  $-\text{CH}=\text{N}-$  group. The peaks at  $1576$  and  $1511\text{ cm}^{-1}$  are due to aromatic ring skeletal vibration and the olefinic  $\text{C}=\text{C}$  stretching, respectively.

The methoxy,  $-\text{OCH}_3$  stretching is positioned at  $2857\text{ cm}^{-1}$ . The para disubstituted nature of aromatic rings is evident by the bending mode of aromatic ring hydrogens at  $808\text{ cm}^{-1}$ . The peak of  $3423\text{ cm}^{-1}$  and  $3550\text{ cm}^{-1}$  can be assigned to hydroxyl,  $-\text{OH}$  group and aromatic amine are also found in the spectrum. CdS is Raman active [13] and could not be observed in the FT-IR spectra.

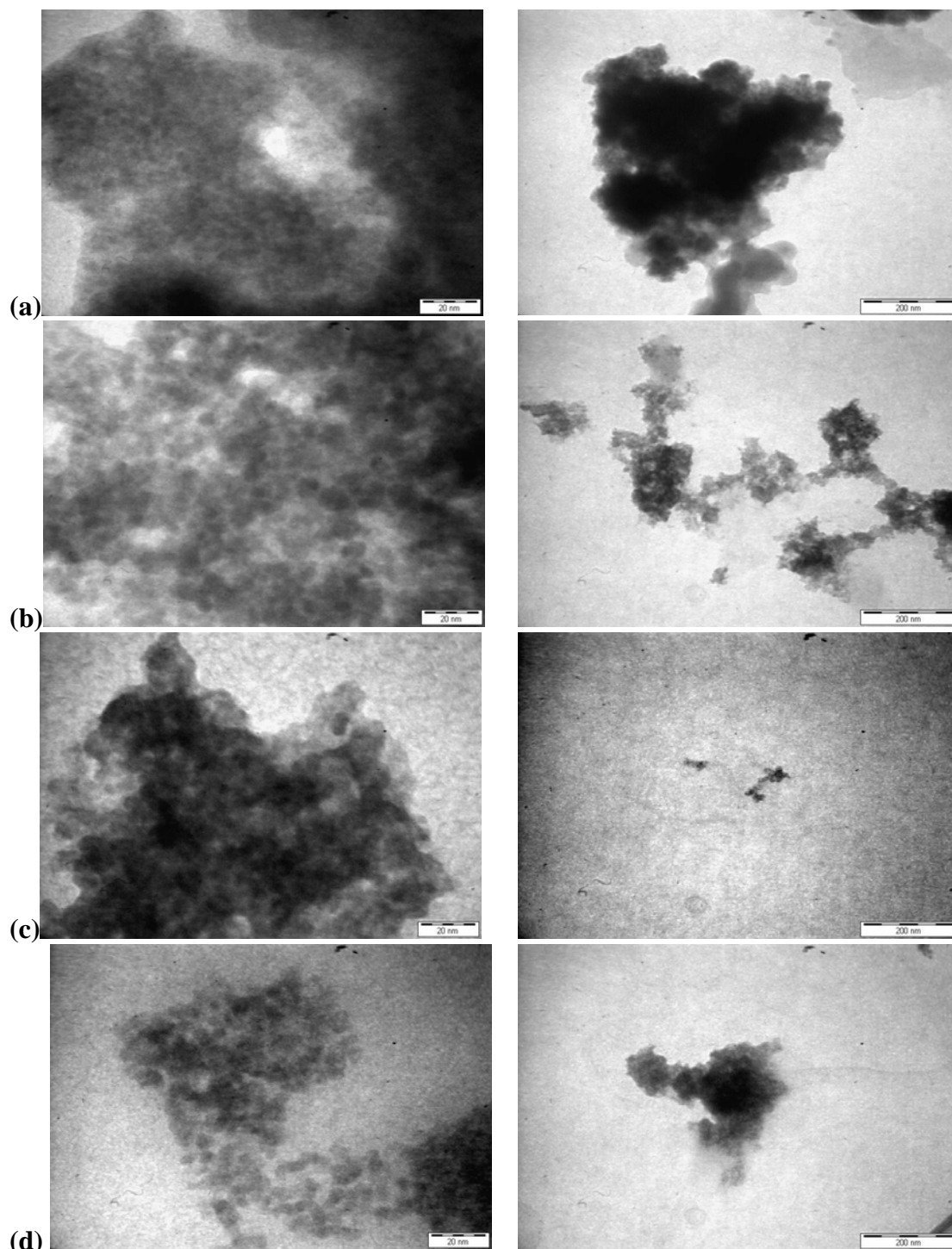
The spectra of nanocomposites at 0.2: 1.0 (w/w) and beyond show a change of peak intensity in the range  $3423\text{--}3550\text{ cm}^{-1}$ . When 30% of CdS composition is introduced in the samples, the peak intensity at  $3550\text{ cm}^{-1}$  has developed stronger whereas the peak at  $3423\text{ cm}^{-1}$  becomes weaker. However, when more CdS is added in the samples, the peak intensity at  $3423\text{ cm}^{-1}$  became more apparent compared to the nanocomposites at the mass composition of 0.2: 1.0 till 0.4:1.0. The peak subsequently becomes broader and only one peak is observed at  $3428\text{ cm}^{-1}$  when the nanocomposites at the mass composition of 0.8: 1.0 up to 1.0:1.0 (w/w). The

changes are due to the physical interaction of CdS with the  $-\text{OH}$  group or the aromatic amines that present in the diol vanillin. Besides that, there is a shift for peak positioned at  $1271\text{ cm}^{-1}$ , which is assigned to the  $-\text{C}-\text{O}-\text{C}-$  stretching. This peak is shifted from  $1271\text{ cm}^{-1}$  to  $1265\text{ cm}^{-1}$  and consequently to  $1260\text{ cm}^{-1}$  when the mass composition is 0.8:1.0 and 1.0:1.0 respectively. These results are attributed to the interaction of CdS with  $-\text{OCH}_3$  group in diol vanillin. Otherwise, the rest of the peaks in the FT-IR spectra remain unchanged.

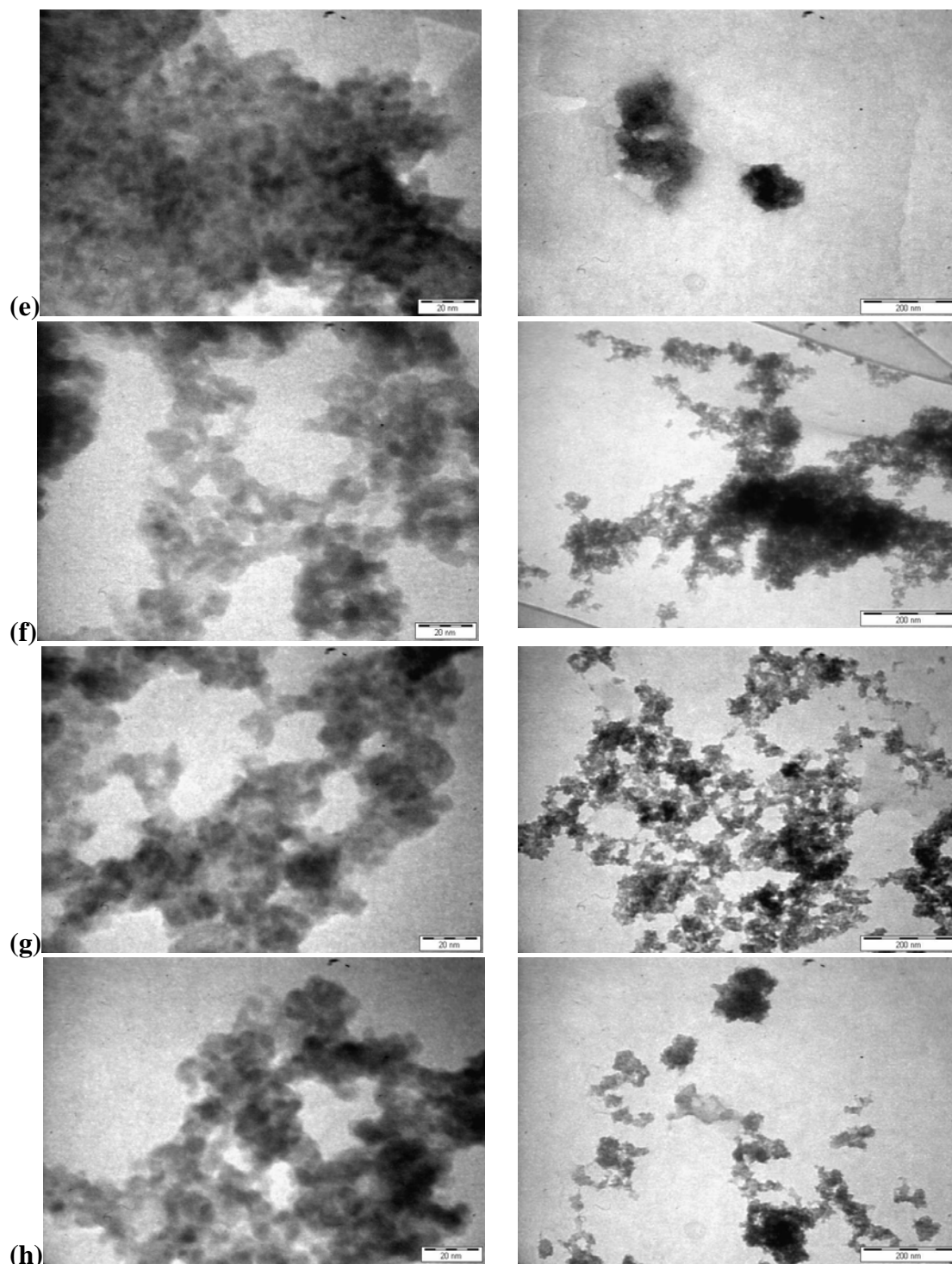
Typical TEM images of the as-prepared nanocomposites at various mass compositions are shown in Fig 5. TEM analyses show that the presence of diol vanillin control the size of the CdS nanoparticles in all the mass composition of the nanocomposites. The TEM micrographs show that the particles are distinguishable and thus, they are not aggregated into a big particle. The average particle size and standard deviation obtained are tabulated in Table 1. The average particle is in consistent size and has irregular rounded shape. The average size of CdS in all the nanocomposites, except for the sample with mass composition of 0.4:1.0, is less than  $4.0\text{ nm}$  with the standard deviation of  $\leq 1.0\text{ nm}$ . The average particle size is smaller than that of as-prepared CdS without diol-vanillin where the as-prepared CdS's average size is  $6.3 \pm 1.1\text{ nm}$ . Figure 6 shows the size distribution of selected mass composition of nanocomposites are in the range of  $3.0\text{--}4.0\text{ nm}$  which unlike the as-prepared CdS that falls in the broader range of  $5.0\text{--}7.0\text{ nm}$ .

Table 1. Average particle size and standard deviation of the prepared nanocomposites at various mass compositions (w/w) of CdS: diol vanillin.

Nanocomposite (w/w)	(Average size + SD) nm
0.1: 1.0	$3.8 \pm 0.9$
0.2:1.0	$3.3 \pm 0.7$
0.3:1.0	$3.8 \pm 0.7$
0.4:1.0	$4.2 \pm 0.8$
0.5:1.0	$3.7 \pm 1.0$
0.6:1.0	$3.7 \pm 0.7$
0.8:1.0	$3.8 \pm 0.7$
1.0:1.0	$3.8 \pm 0.7$



**Fig 5.** TEM micrographs of the as-prepared nanocomposites (CdS: diol vanilin) w/w at various mass compositions (a) 0.1:1.0 (b) 0.2:1.0 (c) 0.3:1.0 (d) 0.4:1.0 (e) 0.5 :1.0 (f) 0.6:1.0 (g) 0.8:1.0 (h) 1.0:1.0 (continued to next page).



**Fig 5 (cont.).** TEM micrographs of the as-prepared nanocomposites (CdS: diol vanilin) w/w at various mass compositions (a) 0.1:1.0 (b) 0.2:1.0 (c) 0.3:1.0 (d) 0.4:1.0 (e) 0.5 :1.0 (f) 0.6:1.0 (g) 0.8:1.0 (h) 1.0:1.0

### Thermal and optical behaviour

The phase transition temperatures of the nanocomposites are presented in Table 2. The melting ( $T_m$ ) and isotropization ( $T_i$ ) points is clearly identifiable from DSC thermograms. The DSC heating scan of

nanocomposites at various mass compositions show two endothermic peaks: a greater intensity peak is assigned from solid to mesophase transition while the smaller peak is assigned from mesophase transition to isotropic phase respectively.

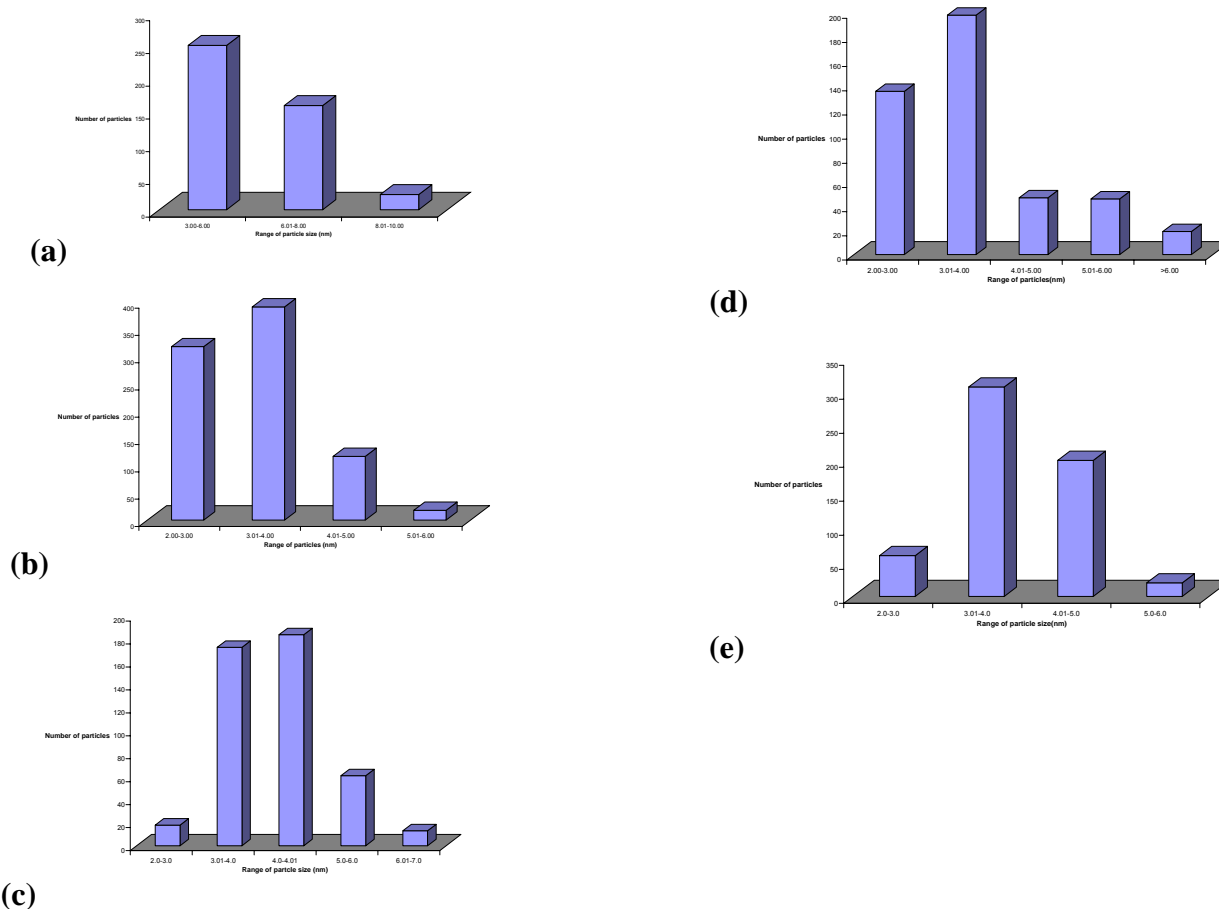


**Fig 6.** Histogram of size distribution of (a) CdS particles and CdS particles in the nanocomposites (CdS: diol vanilin) at different mass composition (w/w) (b) 0.2:1.0 (c) 0.4:1.0 (d) 0.5:1.0 (e) 1.0:1.0

**Table 2.** Transition temperatures of CdS: diol vanilin nanocomposites (at different mass composition.

Nanocomposite (w/w) (CdS:diol vanilin)	Transition	Temperature /°C (Peak)	$\Delta T$ /°C ( $\Delta T = T_i - T_m$ )
Pure diol vanilin	Cr-N	171.0	17.7
	N-I	188.7	
0.1: 1.0	Cr-N	170.4	16.6
	N-I	187.0	
0.2:1.0	Cr-N	170.6	15.2
	N-I	185.8	
0.3:1.0	Cr-N	170.5	14.4
	N-I	184.9	
0.4:1.0	Cr-N	166.4	18.6
	N-I	185.0	
0.5:1.0	Cr-N	168.8	17.2
	N-I	186.0	
0.6:1.0	No transition	168.3	-
0.8:1.0	No transition	-	-
1.0:1.0	No transition	-	-

Cr, crystal; N, nematic; I, isotropic

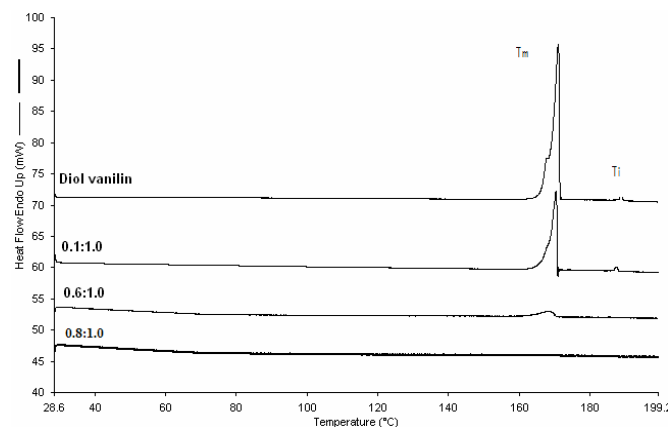


**Fig 7.** DSC thermogram of pure diol vanilin and selected CdS: diol vanillin nanocomposites (CdS: diol vanilin) (0.1:1.0, 0.6:1.0 and 0.8:1.0).

Fig 7. shows the DSC thermogram of pure diol vanilin and selected CdS:diol vanillin . The melting and isotropication points for pure diol vanilin are at 171.0 °C and 188.7 °C respectively. Generally, the introduction of CdS in diol vanillin decreases both the melting and

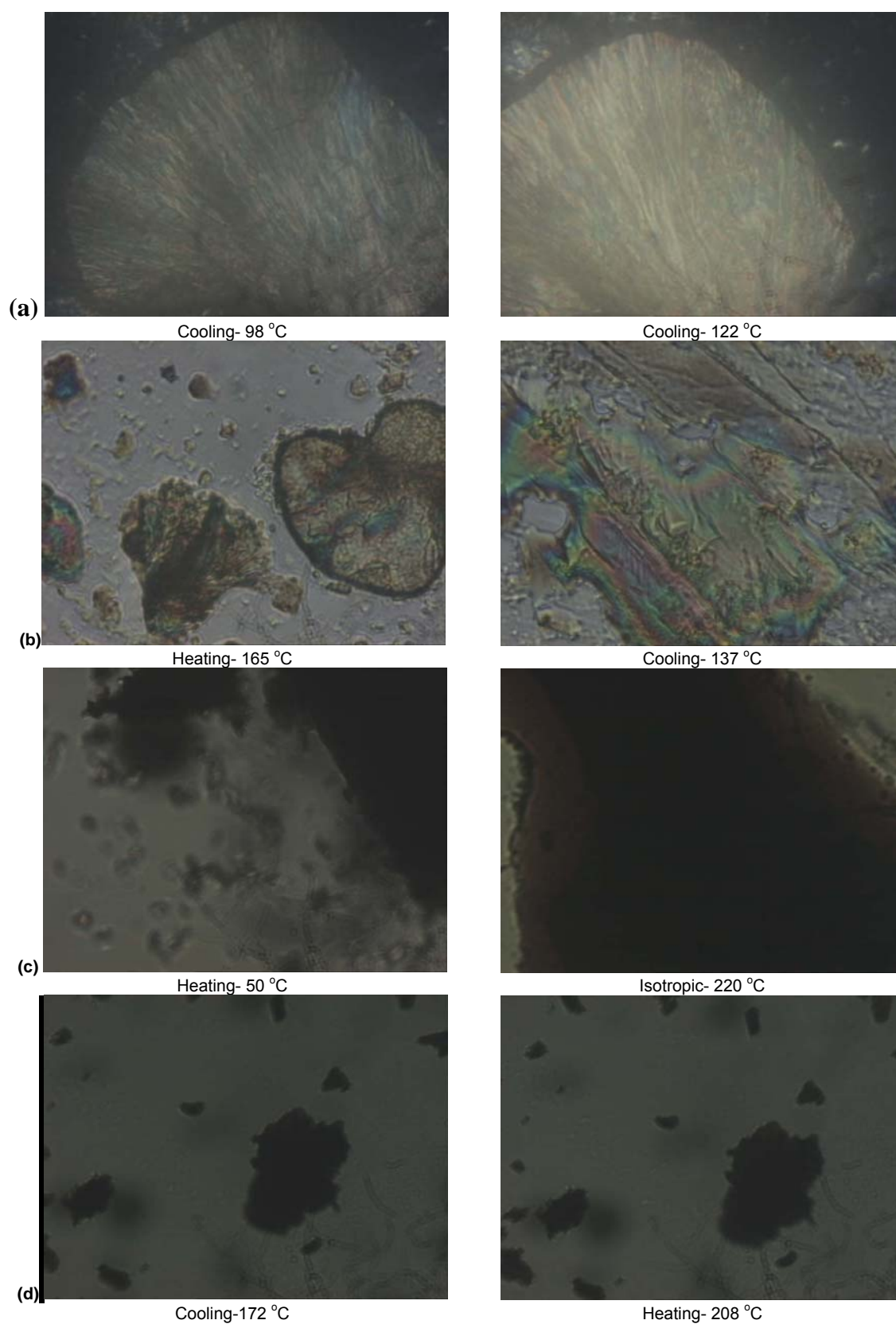


**Fig 8.** POM micrographs of (a) pure diol vanilin and nanocomposites (CdS: diol vanilin) w/w at various temperatures (b) 01:1.0 (c) 0.6:1.0 (d) 0.8:1.0



isotropication insignificantly. A reverse trend is observed for 0.4:1.0 and 0.5:1.0 nanocomposites. The liquid crystal property disappears when the CdS: diol-vanillin mass composition is 0.6:1.0 or greater. Only single melting peak is observed in DSC. When the mass composition is 0.8:1.0 and beyond, no melting point is observed. The mesophase is recognized from the coloured fluidity flow with phase between the crossed polarizers in the microscope exhibited by the nanocomposites. The sample showed Schlieren threaded texture which indicates the nematic mesophase. The obtained nanocomposites are enantiotropic and they are reproducible on repeated heating and cooling cycles. The POM observations correspond well with the DSC obtained results. As observed in the POM micrographs (Figure 8), the dark spots indicate the presence of CdS particles in the samples. When the mass composition of CdS is increased in the sample, the dark spots are more obvious in the micrographs. However, when the mass composition of CdS in the nanocomposite is 0.6:1.0 and beyond, the mesophase of liquid crystal disappears.

## CONCLUSION

The preparation nanocomposites comprising diol vanillin and cadmium sulfide (CdS) is successfully synthesized. The X-ray diffraction pattern (XRD) confirms that the broad peaks are attributed to the formation of cubic CdS nanoparticles in diol vanillin matrix. Introduction of diol vanillin is observed to have control the particle size of CdS in the nanocomposites. The average particle size in all the prepared nanocomposites at different mass composition except sample at 0.4:1.0 (w/w) is less than 4 nm with the standard deviation  $\leq 1.0$  nm. The size distribution for nanocomposites is also narrower compared with that of as-obtained CdS nanoparticles. The analyses from POM and DSC reveal that mass composition from 0.1: 1.0 up to 0.5:1.0 of CdS in the nanocomposites show their enantiotropic nematic phase. Otherwise, when the mass composition of CdS in nanocomposite at 0.6: 1.0 and greater, the liquid crystal property is affected.

## ACKNOWLEDGEMENT

This research is supported in part by Malaysia Toray Scientific Foundation (MTSF) Science and Technology Grant 2005 (304/PKimia/650343/T102) and USM short term grant (304/PKimia/638035).

## REFERENCES

1. Liu, S.H., Qian, A.X.F., Yin, J., Ma, X.D., Yuan, J.Y., and Zhu, Z.K., 2003, *J. Phys. & Chem. Solids*, 64, 544-458.
2. Favero, P.P., Souza-Parise, M.D., Fernandez, J.L.R., and Miotto, R., 2006, *Braz. J. Phys.*, 36(3B), 1032-1034.
3. Sedaghat, Z., Taghavinia, N., and Marandi, M., 2006, *Nanotechn.*, 17, 3812-3816.
4. Nosaka, Y., Yamaguchi, K., Kuwabara, A., Miyama, H., Baba, R., and Fujishima, A.J., 1992, *Photochem. & Photobiol. A: Chem.*, 64(3), 375-382.
5. Murakoshi, K., Hosokawa, H., Saitoh, M., Wada, Y., Sakata, T., Mori, H., Satoh, M., and Yanagida, S., 1998, *J. Chem. Soc., Faraday Trans.*, 94(5), 579-586.
6. El-Tantawy, F., Abdel-Kader, K.M., Kaneko, F., and Sung, Y.K., 2004, *Eur. Polym. J.*, 40(2), 415-430.
7. Wang, Y., and Herron, N., 1992, *Chem. Phys. Lett.*, 200(1-2), 71-75.
8. Antolini, F., Pentimalli, M., Di Luccio, T., Terzi, R., Schioppa, M., Re, M., Mirengi, L., and Tapfer, L., 2005, *Mater. Lett.*, 59(24-25), 3181-3187.
9. Chang, J.-H., Seo, B.-S., and Hwang, D.-H., 2002, *Polymer*, 43(10), 2969-2974.
10. Huang, W., and Han, C.D., 2006, *Polymer*, 47(12), 4400-4410.
11. Khiew, P.S., Huang, N.M., Radiman, S., and Ahmad, M.S., 2004, *Mater. Lett.*, 58(3-4), 516-521.
12. Khiew, P.S., Radiman, S., Huang, N.M., and Soot M., 2003, *J. Cryst. Growth*, 254(1-2), 235-243.
13. Nandakumar, P., Vijayan, C., Rajalakshmi, M., Arora, A.K., and Murti, Y.V.G.S., 2001, *Phys. E: Low-dimensional Syst. & Nanostruct.*, 11(4), 377-383.